Section: Research Paper

A Mathematical study of Hall and Ion slip impacts on Peristaltic transport of hydromagnetic flow through a porous medium with chemical reaction

R.VijayaKumar[1] , A. Jancy Rani2

[1]Mathematics Section, FEAT, Annamalai University, Tamilnadu, India
Department of Mathematics, Periyar Government Arts College,
Cuddalore, Tamilnadu, India

[2]Research Scholar, Department of Mathematics,Annamalai University,
Tamilnadu, India

[1]E-mail address of Presenter for Correspondence: rathirath_viji@yahoo.co.in

Abstract: The scrutinization of the current work deals blood flow in the lopsided wavy channel with chemical reaction in the porous material. The hypothesis of the work can be unsteady, incompressible, mixed convection flow on MHD. Also induced heat transfer surmised due to radiation and analyzed temperature difference from the channel. Thus, impact of parameter for hall and ion slip, Biot number for heat and mass transfer are taken into account. A magnetic effect is functioned uniformly through the channel in the perpendicular direction. The dimensionless governing equations are answered logically in perturbation technique. The critical out comes have been presented graphically.

Keywords: Casson fluid, MHD, Biot number, Hall and Ion slip effect.

1. Introduction

Blood flow plays vital role in human body with distinct situations. Flow direction may be occurred according to the structure of the parts of body. It carries out numerous types of functions as transporting nutrients and oxygen for their digestion, negative carbon dioxide emissions, keeping digestive system normal. The elements of micro-circulation composed of arterioles, capillaries and venules. Varies field researches shows their interest in doing research on blood as non-Newtonian fluid during the past few years. The progress of peristaltic drives biofluid forward by manner of sinusoidal waves which proceed axially besides the length of the channel. It resembles the functioning mode of our body which pumps blood, nutrition and oxygen.

John R. Keltner [1]studied blood flow on MHD in 1990. Human vasculature with the pressure of hydrostatic and electrical effect reacted high on 10 tesla and less as 0.2 percent. Norzieha Mustapha[2] found blood flow in the arteries irregular size multi – stenoses on MHD treating blood as viscous fluid. The author outlined 3D and the flow direction considered as axisymmetric. D.S.Sankar[3]created a method that treats blood as a Casson fluid when the effect of a magnetic field is present in blood flow and narrow arteries. Considering uniform direction as axially symmetric is clearly shown. S.Asghar[4] examined the transportation of peristaltic on MHD fluid through symmetric and asymmetric channels using the hall and ion slip effects. Also heat transportation can be inspected by examining effect of viscous and ohmic dissipation. S.Asghar[5]dealt that certain anatomical fluids as honey, blood, syrups and oils are not true for viscosity fluid as constant also objective of the paper be situated to pass the fluid through peristaltic movement in a symmetric channel. M.M.Bhatti[6]examined the blood flow in a expired arteries slip effect proceeding MHD treating blood as Jeffrey fluid model also assuming 2D non – uniform channel is studied. M.M.Bhatti[7]surveyed due to the effects of MHD and partial slip, the peristaltic blood flow of Ree-Eyring fluid in the porous channel is not uniform.. Farhad Ali [8]obtained the blood flow in place of a Casson fluid model with the effect of magnetohydrodynamics in a horizontal cylinder. The magnetic particles distributed uniformly in the blood. Q.Hussain[9]developed collective effects on hall and ion slip, ohmic dissipation and proceeding peristaltic passage of viscous fluid. Mohammad M.Rashidi[10]analysed the electrical conduction in the magnetic field through the effect of heat and mass transfer. It proceeded blood flow instead of Casson fluid model using peristaltic movement. S. Maiti[11]considered blood flow on MHD modelled by Caputo – Fabrizio fractional order transferring heat and mass in the unidirectional through porous material have an effect on thermal radiation treating blood as Casson fluid. Asma Khalid [12]studied the blood flow in the carbon nano tubes treated as base material done an oscillating perpendicular plate in the porous medium two types of carbon nano tubes utilised on MHD. Madhusudan Senapati [13]analysed blood flow in on the narrow arteries on slip flow with chemical radiation MHD over permeable stretching sheet in porous material impact of slip condition. S.Das[14]investigated blood flow along with copper (cu) and gold nano particles (AuNps) combined effect of electromagnetic force and hall currents passes through not – uniform endoscopic annulus by wall slip. H.Vaidya[15]exposed blood flow through narrow arteries during surgeries impact of MHD with impact of chemical reaction. Non – uniform geometry with partial slip is considered. M.Anusha Bai [16]investigated under the assumption of long wave length in a planner channel the peristaltic fluid of a hyperbolic angle was inserted through the effect of hall and ion slip. RudraRaviKumar Palegari[17] described the model by using lubrication

approach also dealt peristatic stream of a Newtonian fluid by means of the effect of heat transmission through porous medium in the upright channel asymmetrically.

As for as this paper tells, the movement of peristaltic blood flow through lopsided horizontal wavy channel and the magnetic effect is transported perpendicular to the channel with chemical reaction is analysed. Mass Grashof number, heat transfer Biot number, thermal Grashof number, Prandtl number, and mass transfer Biot number, Schmidt and Nusselt numbers are assumed to invent exact solution of the model. Hence the core motto of this learning to find collective effect of chemical reaction in addition radiation in a lopsided wavy channel with porous material. The momentum, temperature and concentration equations of the blood flow are examined methodically also explained graphically.

2. Mathematical formation of the model

Consider the following assumption to build our present model.

- Electrically passing on, optically thin, radiating, Casson fluid stream in a channel is envisaged.
- The stream is intended to pass through wavy channel with the unsteady motion and the flow is supposed to be incompressible.
- The ordering of the two-dimensional co-ordinate system is directed that x – axis is horizontally straight by the side of the channel walls together with the y – axis is vertically upward in which stream is conducted over porous medium through chemical reaction.
- Peristaltic wave disseminates throughout the length of the walls.
- The transportation of heat and mass throughout the channel wall satisfy convective conditions.
- Fluid flow into the magnetic fieldfunctioned uniformly in the crosswise direction. The physical setup can be drawn for the investigation in the Figure 1.

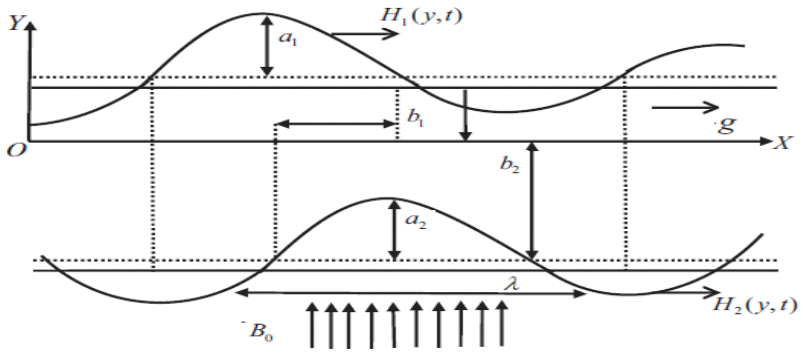

Figure 1.The model's physical setup

Wavy channel intends to permit cross channel collaborating vertical to the direction of the flow as described by P.V.Satya Narayana[18] and T.Hayat[19].

$$H_1 = d_1 + a_1 \cos\frac{2\pi x}{\lambda}$$

$$H_2 = -d_2 - b_1\left(\cos\frac{2\pi x}{\lambda} + \varphi\right) \quad (1)$$

where and satisfy y the condition $a_1^2 + b_1^2 + 2a_1 b_1 \cos\varphi \leq (d_1 + d_2)^2$

In which - upper and lower wall shape a, b – magnitude of the waves, – wavelength, d – width and t – time.

The aspect of differsup on range and corelate with unevenly shaped channel but waves are outside the channel where as that are inside the segment.

The complete physical model can be considered continual of the momentum equation. The peristaltic wave is extended to finite distance. Hence according to the figure, y is function of it. The temperature and concentration are taken as which the fluid is constant. Assuming the above conditions, the governing equations framed.

$$\frac{\partial u}{\partial t} + \tilde{V}\frac{\partial u}{\partial y} = -\frac{1}{\rho}\frac{\partial p}{\partial x} + \nu\left(1 + \frac{1}{\beta}\right)\frac{\partial^2 u}{\partial y^2} - \frac{B_0 J_y}{\rho} + g\beta_T(T - T_1) + g\beta_C(C - C_1) - \frac{\nu}{k}u \quad (2)$$

$$\frac{\partial v}{\partial t} + \tilde{V}\frac{\partial v}{\partial y} = -\frac{1}{\rho}\frac{\partial p}{\partial x} + \nu\left(1 + \frac{1}{\beta}\right)\frac{\partial^2 v}{\partial y^2} - \frac{B_0 J_x}{\rho} - \frac{\nu}{k}v \quad (3)$$

$$\rho C_p\left(\frac{\partial T}{\partial t} + \tilde{V}\frac{\partial T}{\partial y}\right) = K_T\frac{\partial^2 T}{\partial y^2} - \frac{\partial q_r}{\partial y} - Q_0(T - T_1) \quad (4)$$

$$\frac{\partial C}{\partial t} + \tilde{V}\frac{\partial C}{\partial y} = D_m\frac{\partial^2 C}{\partial y^2} - K_C(C - C_1) \quad (5)$$

where u and v be the components of velocities along x and y directions. $\tilde{v}$ – suction velocity, ρ – density of the fluid, g – acceleration due to gravitation, β_T and β_C thermal and concentration expansion coefficient, ν - coefficient of kinematic viscosity, C_p – specific heat capacity, K_T-thermal diffusivity of a

fluid, Q_0 – heat generation/absorption, q_r – radioactive heat flux, T – temperature, C – concentration, D_m – chemical molecular diffusivity, K_C – Chemical reaction.

The dimensional form of boundary conditions

$$t < 0 \quad u = 0, v = 0, T = T_1, C = C_1, \quad \forall y$$

$$t > 0 \quad \frac{\partial u}{\partial y} = \frac{\alpha_f}{\sqrt{K_p}} u, \frac{\partial v}{\partial y} = \frac{\alpha_f}{\sqrt{K_p}} v, \frac{\partial T}{\partial y} = \frac{\alpha_T}{\sqrt{K_p}} (T_1 - T), \frac{\partial C}{\partial y} = \frac{\alpha_c}{\sqrt{K_p}} (C_1 - C) \quad \text{at } y = H_1$$

$$\frac{\partial u}{\partial y} = \frac{\alpha_f}{\sqrt{K_p}} u, \frac{\partial v}{\partial y} = \frac{\alpha_f}{\sqrt{K_p}} v, \frac{\partial T}{\partial y} = \frac{\alpha_T}{\sqrt{K_p}} (T - T_2), \frac{\partial C}{\partial y} = \frac{\alpha_c}{\sqrt{K_p}} (C - C_2) \quad \text{at } y = H_2 \qquad (6)$$

Here α_f - velocity slip parameter, K_p - permeability of the porous material, u – slip velocity, α_c- concentration slip parameter, α_T– thermal slip parameter. Here fluid velocity is considered as slip velocity.

The reduction of the expansion $-\frac{\partial q_r}{\partial y}$ can be assumed either optically thin or optically thick gas. If it is optically thick gas assumption, then it intends strong thermal radiation absorption. Such radiation is mostly released from the outward layer. It can be predicted to pass through the boundary layer. Therefore, aforementioned supposition has not been used. Hence J.R. Pattnaik[20] and W.G. England [21] are expressed as,

$$\frac{\partial q_r}{\partial y} = -4a\sigma(T_1^4 - T^4) \qquad (7)$$

The assumption of the temperature variance within the flow are adequately miniature. The temperature T^4 might be indicated as a linear function. To expand T^4 Tayler series formula can be used, so we get,

$$T^4 \cong 4T_1^3 T - 3T_1^4 \qquad (8)$$

Using equations (7) and (8) in (4), we get

$$\rho C_p \left(\frac{\partial T}{\partial t} + \tilde{V} \frac{\partial T}{\partial y} \right) = K_T \frac{\partial^2 T}{\partial y^2} - 16a\sigma T_1^3 (T - T_1) - Q_0 (T - T_1) \qquad (9)$$

Consider the Casson fluid is sucked continuously the channel walls through the time depending on velocity $\tilde{V}$. That can be in the form referred from I.M.I. Eldesoky[22].

$$\tilde{V} = u_p \left(1 + \varepsilon e^{i\omega t}\right) \qquad (10)$$

Where u_p is uniform transpiration velocity and extension of suction velocity. It is not zero productive constant. is constant and small value which satisfy the constraint $\varepsilon < 1$.

The assumption of electron – atom collision is much. So,Currents of hall and ion slip are considerable. Since the strong point of magnetic become huge,Ohm's law can be made adjustments toward insertion the effect of hall and ion slip [23].

$$J = \sigma(E + q \times B) - \frac{\beta_e}{B_0}(J \times B) + \frac{\beta_e \beta_i}{B_0^2}\big((J \times B) \times B\big) \quad (11)$$

In addition, This can be estimated hall parameter $\alpha_e = \beta_e \sim O(1)$and ion slip parameter $\alpha_i = \beta_e\beta_i << 1$, in Equation By the assumptions electric field (E = 0)[24][25].

Therefore, the equation(11) becomes as

$$(1 + \alpha_i\alpha_e)J_x + \alpha_e J_y = \sigma' B_0 v$$

$$(1+\alpha_i\alpha_e)J_z - \alpha_e J_x = -\sigma' B_0 u \quad (12)$$

Solving the above equations, (11) and (12) We get,

$$J_x = \sigma B_0(\alpha_{22}u + \alpha_{11}v)$$

$$J_y = -\sigma B_0(\alpha_{22}v - \alpha_{11}u) \quad (13)$$

Where $\beta_I = \frac{1+\alpha_e\alpha_i}{(1+\alpha_e\alpha_i)^2+\alpha_e^2}, \beta_{II} = \frac{\alpha_e}{(1+\alpha_e\alpha_i)^2+\alpha_e^2}$

Substituting the above Equ (13) in (2) and (3) we acquire as

$$\frac{\partial u}{\partial t} + \tilde{V}\frac{\partial u}{\partial y} = -\frac{1}{\rho}\frac{\partial p}{\partial x} + \nu\left(1+\frac{1}{\beta}\right)\frac{\partial^2 u}{\partial y^2} - \frac{\sigma B_0^2(\beta_I v + \beta_{II}u)}{\rho} + g\beta_T(T-T_1) + g\beta_C(C-C_1) - \frac{\nu}{k}u \quad (14)$$

$$\frac{\partial v}{\partial t} + \tilde{V}\frac{\partial v}{\partial y} = -\frac{1}{\rho}\frac{\partial p}{\partial y} + \nu\left(1+\frac{1}{\beta}\right)\frac{\partial^2 v}{\partial y^2} - \frac{\sigma B_0^2(\beta_I u + \beta_{II}v)}{\rho} - \frac{\nu}{k}v \quad (15)$$

Combining equations (14) and (15) Let $q_f = U + iV$, $\xi = x - iy$ *and* $-\frac{\partial p}{\partial \xi} = \lambda e^{i\omega t}$ we acquire the below equation.

$$\frac{\partial q}{\partial t} + \tilde{V}\frac{\partial q}{\partial y} = -\frac{1}{\rho}\frac{\partial p}{\partial \xi} + \nu\left(1+\frac{1}{\beta}\right)\frac{\partial^2 q}{\partial y^2} - \frac{\sigma B_0^2(\beta_I + i\beta_{II})}{\rho}q + g\beta_T(T-T_1) + g\beta_C(C-C_1) - \frac{\nu}{k}q \quad (16)$$

Introducing the non – dimensional quantities in the above equations described as:

$$q_f = \frac{q}{u_p}, \eta_f = \frac{y}{d}, x_f = \frac{x}{\lambda}, \bar{t} = \frac{tu_p}{d_1}, \theta = \frac{T-T_1}{T_2-T_1}, \varphi = \frac{C-C_1}{C_2-C_1}, \xi_f = \frac{\xi}{\lambda}, h_2 = \frac{H_2}{d_1}, h_1 = \frac{H_1}{d_1}, d = \frac{d_2}{d_1}, a = \frac{a_1}{d_1}, b = \frac{b_1}{d_1}, p = \frac{d_1^2 P}{\rho\nu u_f \lambda}, \xi = \frac{\mu}{\rho}, \bar{u} = \frac{U}{u_p}, \bar{v} = \frac{V}{u_p}$$

Under dimensionless quantities, governing equations diminish to the next procedures

$$Re\left(\frac{\partial q_f}{\partial t} + \left(1+\varepsilon e^{i\omega t}\right)\frac{\partial q_f}{\partial \eta_f}\right) = \lambda e^{i\omega t} + \left(1+\frac{1}{\beta}\right)\frac{\partial^2 q_f}{\partial \eta_f^2} + G_r\theta + G_m\varphi - (M^2(\beta_I + i\beta_{II}) + \sigma^2)q_f \quad (17)$$

$$Re\left(\frac{\partial \theta}{\partial t} + \left(1+\varepsilon e^{i\omega t}\right)\frac{\partial \theta}{\partial \eta_f}\right) = \frac{1}{P_r}\frac{\partial^2 \theta}{\partial \eta_f^2} - (R+Q)\theta \quad (18)$$

$$Re\left(\frac{\partial \varphi}{\partial t} + \left(1+\varepsilon e^{i\omega t}\right)\frac{\partial \varphi}{\partial \eta_f}\right) = \frac{1}{S_c}\frac{\partial^2 \varphi}{\partial \eta_f^2} - K_C\varphi \quad (19)$$

where, $q_f = U + i\,V$, $R_e = \frac{u_p a_1}{\nu}$ – Reynolds number, $G_r = \frac{a_1^2 g\beta_C(T_2-T_1)}{u_p\nu}$ – Thermal Grashof number, $G_m = \frac{d_1^2 g\beta_c(C_2-C_1)}{u_n\nu}$ – Mass Grashof number, $M^2 = \frac{\sigma B_0^2 d_1^2}{u}$ – Squared Hartmann number, $\sigma^2 = \frac{d_1^2}{k}$ – Porous Parameter, $P_r = \frac{\rho C_p \nu}{K_T}$ – Prandtl number, $R = \frac{16a\sigma T^3 d_1^2}{\rho C_p \nu}$–Radiation parameter, $Q = \frac{Q_0 d_1^2}{\rho C_p \nu}$ – Heat generation parameter, $S_c = \frac{\nu}{D}$– Schmidt number, $K_C = \frac{K_c d_1^2}{\nu}$ – Chemical reaction parameter.

The non - dimensional form of boundary conditions

$t < 0, q_{f=0,} \theta = 0, \varphi = 0 \qquad \forall y_f$

$t > 0, \frac{\partial q_f}{\partial \eta_f} = \alpha_f \sigma q_f, \frac{\partial \theta}{\partial \eta_f} = B_h \theta, \frac{\partial \varphi}{\partial \eta_f} = B_m \varphi \quad \text{at } \eta_f = h_1$

$$\frac{\partial q_f}{\partial \eta_f} = -\alpha_f \sigma q_f, \frac{\partial \theta}{\partial \eta_f} = B_h(1-\theta), \frac{\partial \varphi}{\partial \eta_f} = B_m(1-\varphi) \quad \text{at } \eta_f = h_2 \tag{20}$$

Where $B_h = \frac{\alpha_h d}{K_d}$ – Heat transfer biot number, $B_m = \frac{\alpha_m d}{K_m}$ – Mass transfer biot number

3. Method of Solution

Using perturbation method, the velocity, temperature and concentration are considered to receive exact solution.

$$q_f(z,t) = q_{f_0}(z) + \varepsilon e^{i\omega t} q_{f_1}(z) + O(\varepsilon^2), \tag{21}$$
$$\theta(z,t) = \theta_0(z) + \varepsilon e^{i\omega t} \theta_1(z) + O(\varepsilon^2), \tag{22}$$
$$\varphi(z,t) = \varphi_0(z) + \varepsilon e^{i\omega t} \varphi_1(z) + O(\varepsilon^2) \tag{23}$$

For the sake of solving the equations (17), (18) and (19) following pressure gradient assumed to solve velocity, temperature and concentration.

$$-\frac{\partial p}{\partial \xi} = \lambda e^{i\omega t} \; and \; f(\eta_f, t) = f_0(\eta_f) + \epsilon e^{i\omega t} f_1(\eta_f) + o(\epsilon^2) \tag{24}$$

where f is the q_f, θ and φ, f_0 is the q_{f_0}, θ_0 and φ_0 , f_1 is the q_{f_1}, θ_1 and φ_1

Zeroth order equations

$$q_{f_0} = A_9 e^{m_9 \eta_f} + A_{10} e^{-m_{10} \eta_f} + S_{37} + S_{38} e^{m_5 \eta_f} + S_{39} e^{-m_6 \eta_f} + S_{40} e^{m_1 \eta_f} + S_{41} e^{-m_2 \eta_f} \tag{25}$$

$$\theta_0 = A_1 e^{m_1 \eta_f} + A_2 e^{-m_2 \eta_f} \tag{26}$$

$$\varphi_0 = A_5 e^{m_5 \eta_f} + A_6 e^{-m_6 \eta_f} \tag{27}$$

First order equations

$$q_{f_1} = A_{11} e^{m_{11} \eta_f} + A_{12} e^{-m_{12} \eta_f} + S_{54} e^{m_9 \eta_f} - S_{55} e^{-m_{10} \eta_f} - S_{56} e^{m_7 \eta_f} - S_{57} e^{-m_8 \eta_f} - S_{58} e^{m_3 \eta_f} + S_{59} e^{m_5 \eta_f} - S_{60} e^{-m_6 \eta_f} + S_{61} e^{m_1 \eta_f} - S_{62} e^{-m_2 \eta_f} \tag{28}$$

$$\theta_1 = A_3 e^{m_3 \eta_f} + A_4 e^{-m_4 \eta_f} + S_{20} e^{m_1 \eta_f} + S_{21} e^{-m_2 \eta_f} \tag{29}$$

$$\varphi_1 = A_7 e^{m_7 \eta_f} + A_8 e^{-m_8 \eta_f} + S_{12} e^{m_5 \eta_f} + S_{13} e^{-m_6 \eta_f} \tag{30}$$

Subject to the boundary conditions

$$\left\{\frac{\partial q_{f_0}}{\partial \eta_f} = \alpha_f \sigma q_{f_0}, \text{at } \eta_f = h_1\right\}$$

$$\left\{\frac{\partial \theta_0}{\partial \eta_f} = B_h \theta_0 \text{at } \eta_f = h_1, \quad \frac{\partial \theta_0}{\partial \eta_f} = B_h(1-\theta) \text{ at } \eta_f = h_2\right\}$$

$$\left\{\frac{\partial \varphi_0}{\partial \eta_f} = B_m \varphi \text{ at } \eta_f = h_1, \frac{\partial \varphi_0}{\partial \eta_f} = B_m(1-\theta) \text{at } \eta_f = h_2\right\} \quad (31)$$

$$\left\{\frac{\partial q_{f_1}}{\partial \eta_f} = \alpha_f \sigma q_{f_1} \text{at } \eta_f = h_1\right\}$$

$$\left\{\frac{\partial \theta_1}{\partial \eta_f} = B_h \theta_1 \text{at } \eta_f = h_1, \frac{\partial \theta_1}{\partial \eta_f} = -B_h \theta_1 \text{at } \eta_f = h_2\right\}$$

$$\left\{\frac{\partial \varphi_1}{\partial \eta_f} = B_m \varphi_1 \text{ at } \eta_f = h_1, \frac{\partial \varphi_1}{\partial \eta_f} = -B_m \varphi_1 \text{ at } \eta_f = h_2\right\} \quad (32)$$

Answering first order equations are derived via perturbation series. The equations (25) – (30) in equation (31) – (32) with corresponding boundary conditions are substituted.

$$q_f = A_9 e^{m_9 \eta_f} + A_{10} e^{-m_{10} \eta_f} + S_{37} + S_{38} e^{m_5 \eta_f} + S_{39} e^{-m_6 \eta_f} + S_{40} e^{m_1 \eta_f} + S_{41} e^{-m_2 \eta_f} + \varepsilon e^{i\omega t}(A_{11} e^{m_{11} \eta_f} + A_{12} e^{-m_{12} \eta_f} + S_{54} e^{m_9 \eta_f} - S_{55} e^{-m_{10} \eta_f} - S_{56} e^{m_7 \eta_f} - S_{57} e^{-m_8 \eta_f} - S_{58} e^{m_3 \eta_f} + S_{59} e^{m_5 \eta_f} - S_{60} e^{-m_6 \eta_f} + S_{61} e^{m_1 \eta_f} - S_{62} e^{-m_2 \eta_f}) \quad (33)$$

$$\theta = A_1 e^{m_1 \eta_f} + A_2 e^{-m_2 \eta_f} + \varepsilon e^{i\omega t}(A_3 e^{m_3 \eta_f} + A_4 e^{-m_4 \eta_f} + S_{20} e^{m_1 \eta_f} + S_{21} e^{-m_2 \eta_f}) \quad (34)$$

$$\varphi = A_5 e^{m_5 \eta_f} + A_6 e^{-m_6 \eta_f} + \varepsilon e^{i\omega t}(A_1 e^{m_7 \eta_f} + A_8 e^{-m_8 \eta_f} + S_{12} e^{m_5 \eta_f} + S_{13} e^{-m_6 \eta_f}) \quad (35)$$

Skin Friction

The dimensionless structure of Skin friction on porous channel can be specified through:

$$\tau = e^{m_5 \eta_f} m_5 S_{38} - e^{-m_6 \eta_f} m_6 S_{39} + e^{m_1 \eta_f} m_1 S_{40} - e^{-m_2 \eta_f} m_2 S_{41} - e^{-m_{10} \eta_f} m_{10} A_{10} + e^{it\omega} \varepsilon (e^{m_5 \eta_f} m_5 S_{12} - e^{-m_6 \eta_f} m_6 S_{13} + e^{m_{11} \eta_f} m_{11} A_{11} - e^{-m_{12} \eta_f} m_{12} A_{12}) + e^{m_9 \eta_f} m_9 A_9$$

Nusselt Number

$$Nu = e^{m_1 \eta_f} m_1 A_1 - e^{-m_2 \eta_f} m_2 A_2 + e^{it\omega} \varepsilon (e^{m_1 \eta_f} m_1 S_{20} - e^{-m_2 \eta_f} m_2 S_{21} + e^{m_3 \eta_f} m_3 A_3 - e^{-m_4 \eta_f} m_4 A_4)$$

Sherwood Number

The non-dimensional structure of mass transfer in term of Sh is stated through:

$$Sh = e^{m_5 \eta_f} m_5 A_5 - e^{-m_6 \eta_f} m_6 A_6 + e^{it\omega} \varepsilon (e^{m_5 \eta_f} m_5 S_{12} - e^{-m_6 \eta_f} m_6 S_{13} + e^{m_7 \eta_f} m_7 A_7 - e^{-m_8 \eta_f} m_8 A_8)$$

4. Results and Discussions:

In the process of graphical depiction velocity, temperature, concentration, Sherwood number, Nusselt number Nu and Wall shear stress be computed

then graphically presented the consequences of various flow parameters. Velocity profiles are represented in the Figures 2.1 – 2.8. Temperature profiles are demonstrated in the Figure from 3.1 – 3.4whereas concentration profiles are shown in the Figure from 4.1 – 4.3. Wall shear stress , Nusselt number Nu and Sherwood number Sh profiles are displayed in the Figures from 5.1 – 5.4, 6.1 – 6.4 and 7.1 – 7.2. For the purpose of computation, we fix the system parameters values as $\varepsilon = 0.1;\ a = 0.7;\ b = 0.8;\ d = 2;\ \varphi = \frac{\pi}{2};\ x = 0.5; t = 0.3$

4.1 The graphical explanation of Velocity:

The velocity U along with velocity V demonstrate the outcome of Hartmann number M in Figure 2.1. Here U and V lead to a increment in the velocity since the Hartman number M rises through region. Due to increase in Hartman number velocity increase up to the certain number. Since mounting M tending the drag force to rise and that causes the fluid movements to delay in which the result augmented drag force which is equal the drag force by the effect of magnetic on an electrically passing fluid yield resistive force.

Figures 2.2, 2.3 and 2.4 portrayed the displacement of velocity U and V through hall effect, radiation and heat generation parameters. This is notified that as supplementation in hall effect, radiation and heat generation the velocity U decreases through the area though it is observed the velocity V augments by means of the rising in hall effect, radiation and heat generation. Since producing the effects which results increase the resultant speed and enlargement in the momentum layer thickness throughout the fluid area.

Ion slip effect, chemical reaction and mass Grashof number Gm can be graphically exposed in the Figures 2.5,2.6 and 2.7. The velocity U progresses and velocity V diminishes with mounting in ion slip effect, chemical reaction and mass Grashof number Gm all over the region. The mass Grashof number Gm ion slips effect, chemical reaction and mass Grashof number Gm boost by the advantage of strengthening of the effects. The distribution of velocity expands swiftly go to next level of porous medium later reduces for the stream quantity. Hence increase in ion slip effect, chemical reaction and mass Grashof number Gm the boundary layer thinness augment.

Thermal Grashof number Gr be displayed in the Figure 2.8. Though thermal grashof number Gr increases, it indicates the proportion of current force to the hydromagnetic over the borderline layer the velocity U decreases and velocity V maintained same length in the region.

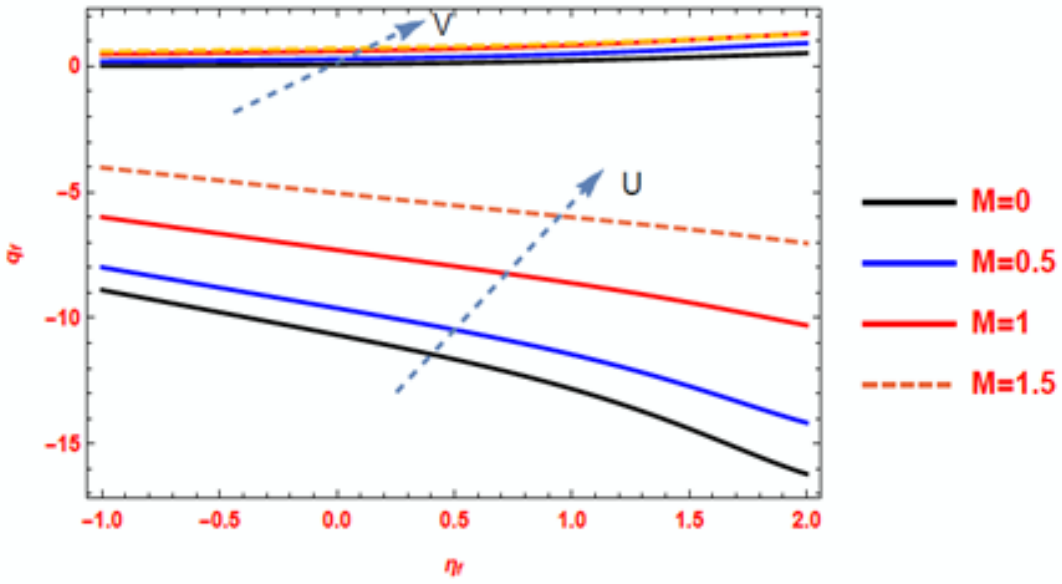

Figure 2.1

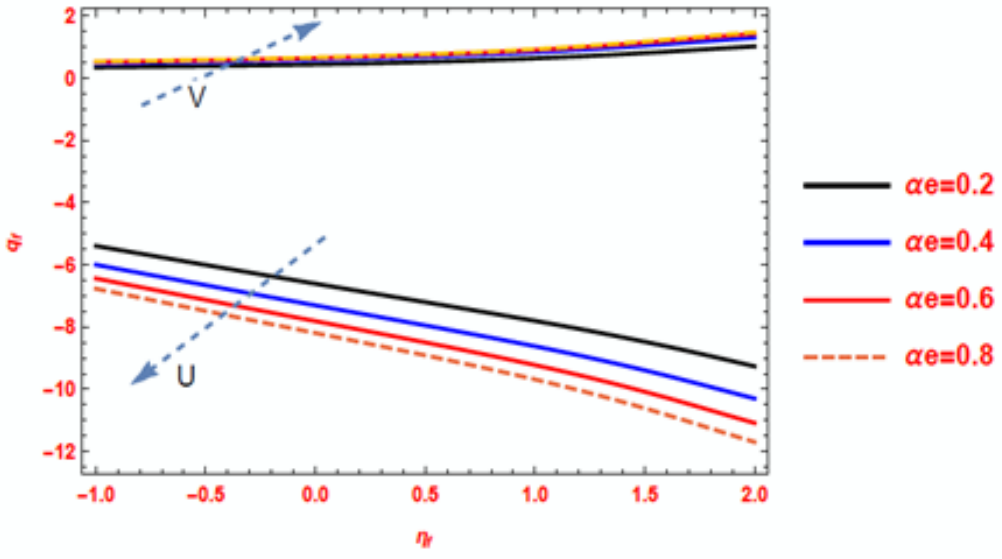

Figure 2.2

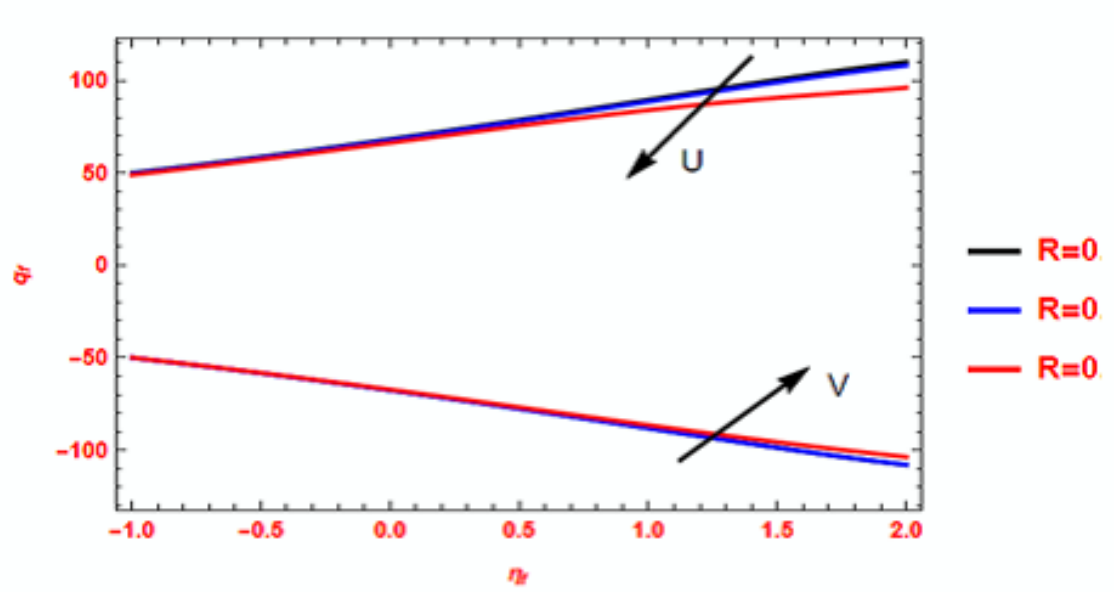

Figure 2.3

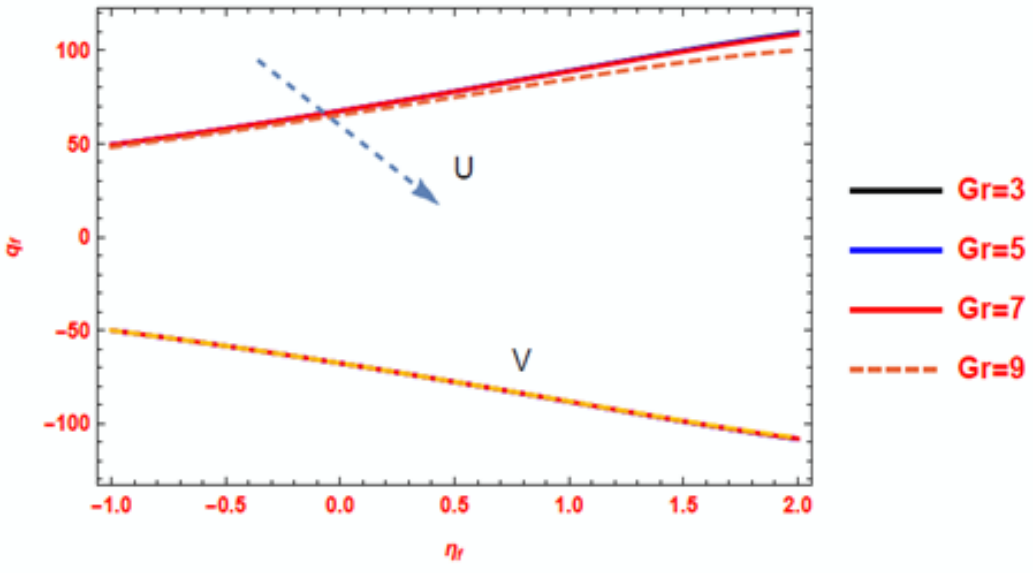

Figure 2.4

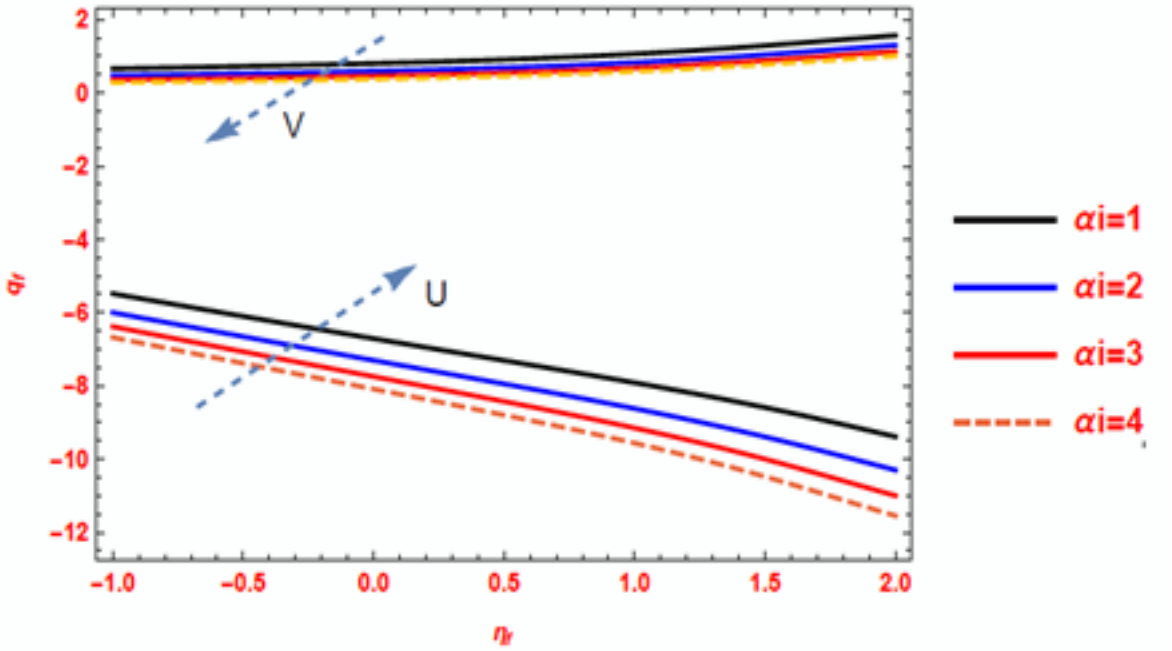

Figure 2.5

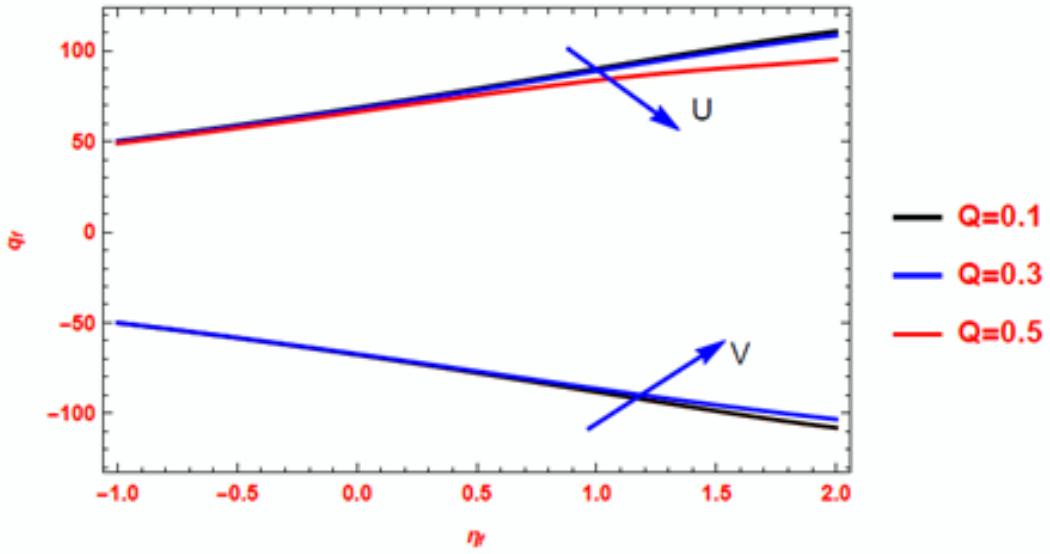

2.5

Figure 2.6

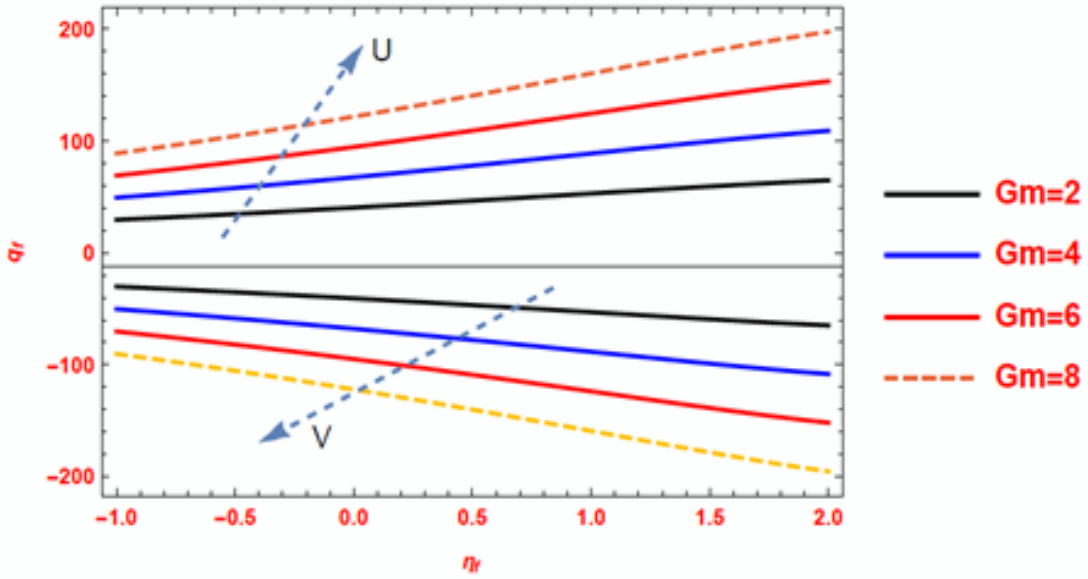

Figure 2.7

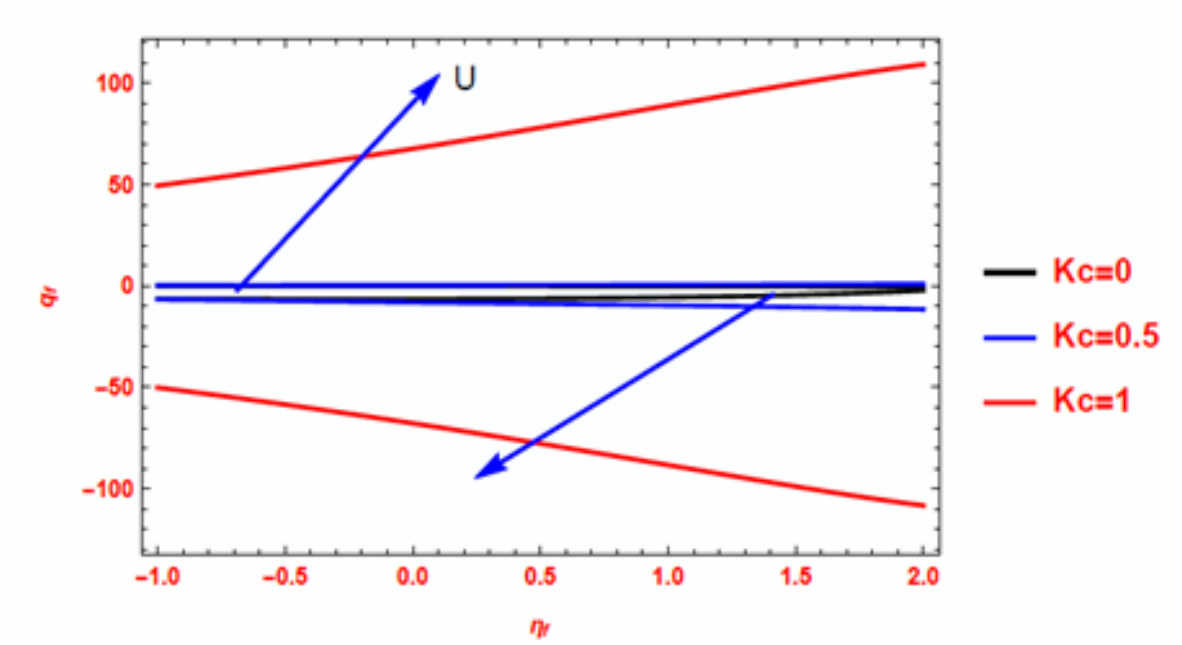

Figure2.8

Effect of $M, \alpha_e, R, Q, \alpha_i, Kc, Gm, Gr$ on Velocity Profile

4.2 The graphical explanation of Temperature θ:

The dissimilar values of temperature like Prandtl number Pr, heat transfer Biot number B_h, parameter for Radiation R and Heat generation Q showed in the Figures 3.1, 3.2, 3.3 and 3.4. Temperature distributions rise in the positive area where as lessening in the negative area with increasing values of heat transfer Biot number, radiation parameter and heat generation parameter only the Prandtl number values have given randomly. This can be due to thermal conductivity of fluid resulting the boundary layer thickness.

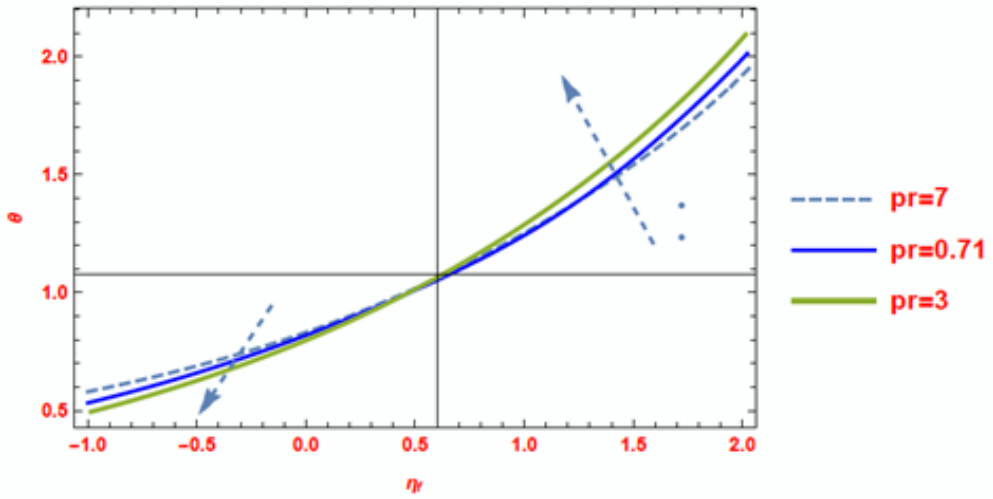

Figure 3.1

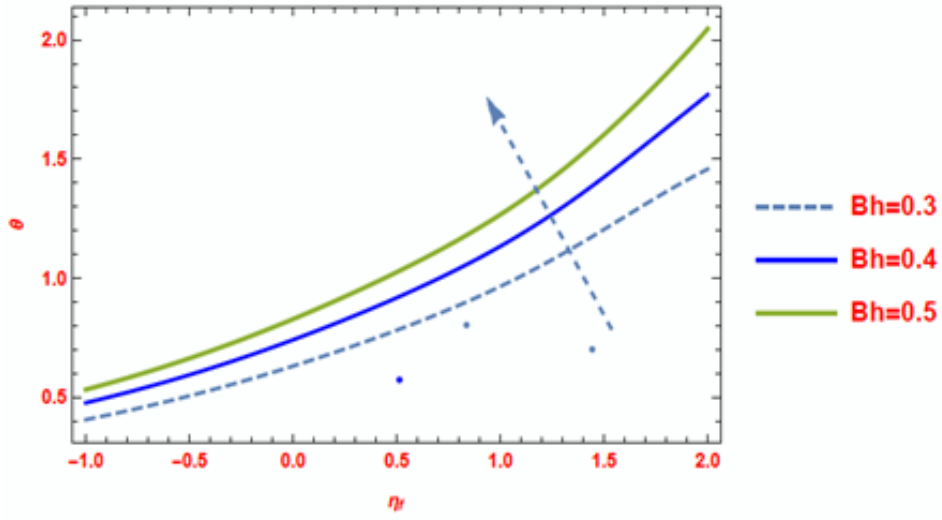

Figure 3.2

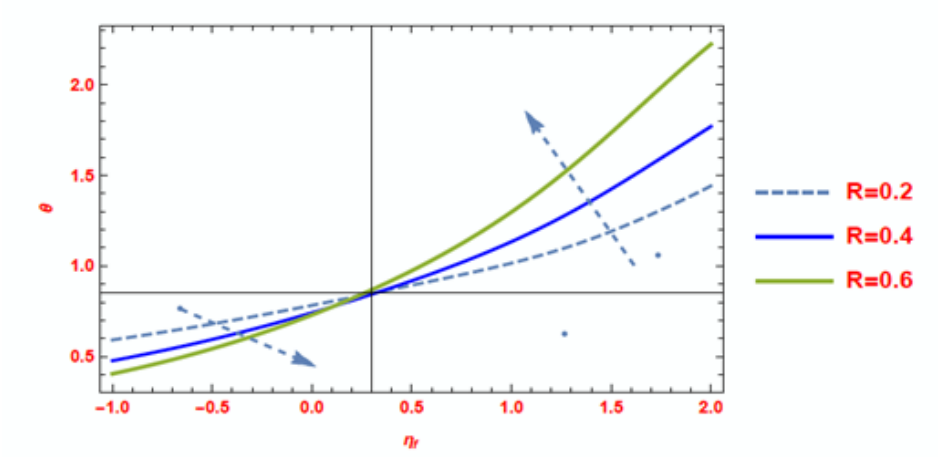

Figure 3.3

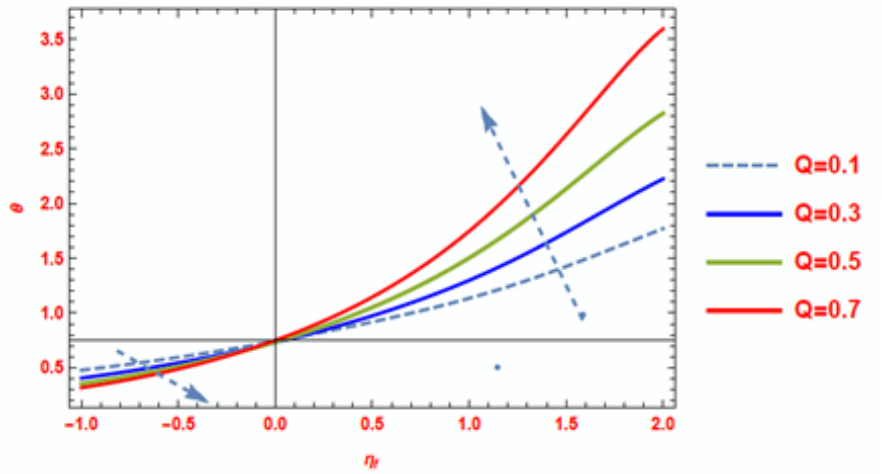

Figure 3.4

4.3 The graphical explanation of Concentration :

Figure 4.1 illustrate Schmidt number as concentration profile. The dimensionless number of Schmidt number Sc can be stated in place of the proportion of momentum diffusivity and mass diffusivity after that these are applied to distinguish fluid flows within there would be momentum, mass diffusion and concentration boundary layers. Hence there is a growth in the rate of Schmidt number brought about the absorption of fluid elements be sides as a consequence the concentration boundary layer thinness to reduce considerably.

Figures 4.2 and 4.3 displayed parameter for Chemical reaction Kc and Biot number form ass transfer Bm as concentration profile. Biot number for mass transfer Bm is a dimensionless number used to calculate the heat transfer and Chemical reaction parameter Kc reduce the heat transfer but then again increase the mass transfer rate. Hence fluid concentration increases in parameter values of Kc and Bm with the with the boundary layer thickness.

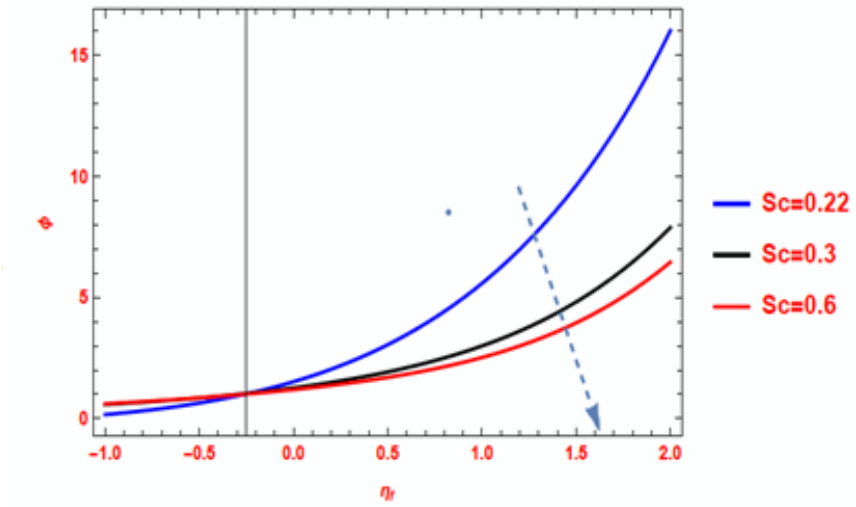

Figure 4.1

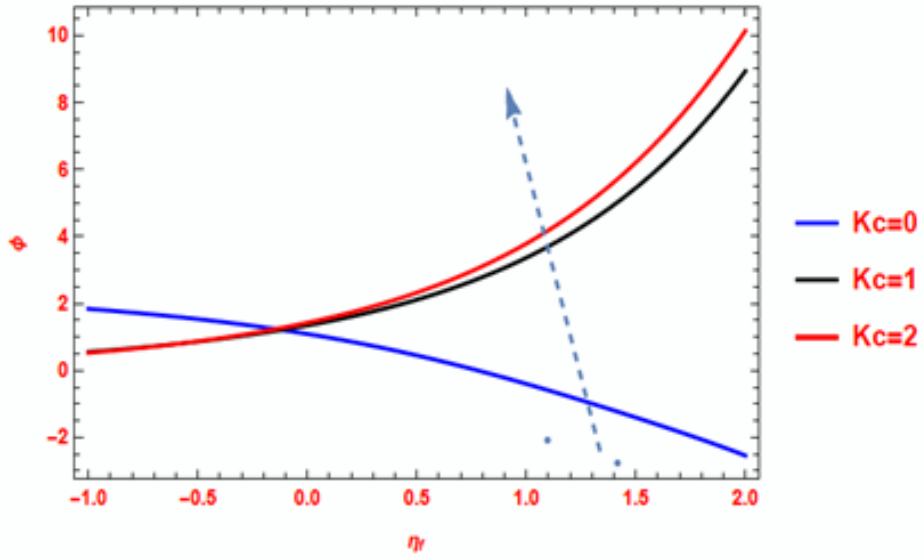

Figure 4.2

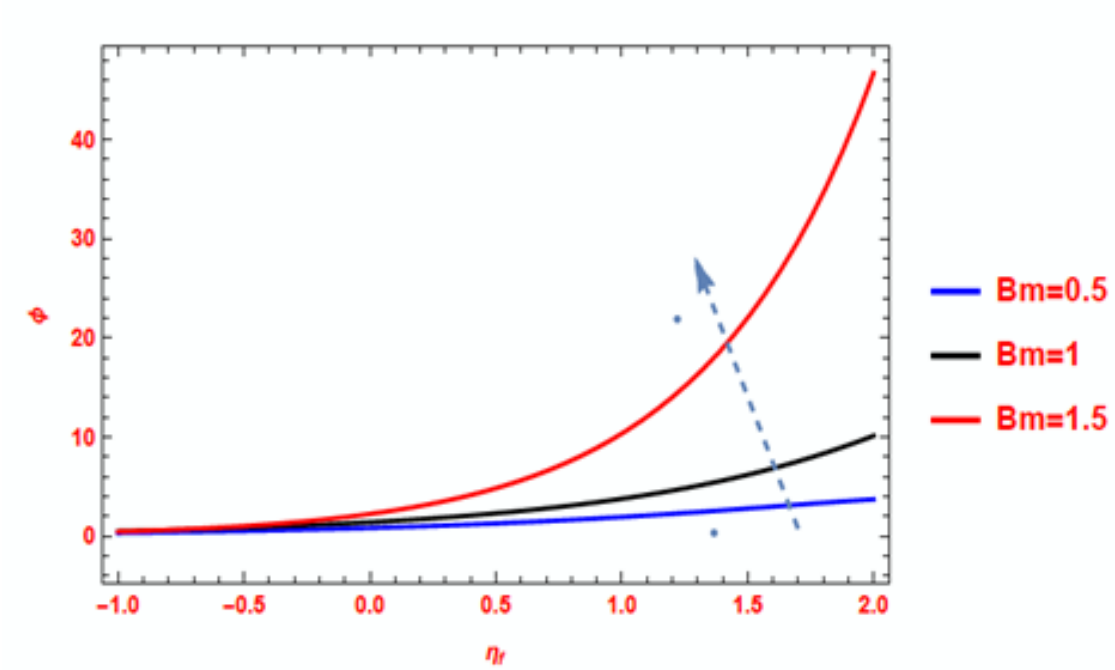

Figure 4.3

Effect of Sc,Kc and Bm on Concentration profile

4.4 The graphical explanation of wall shear stress :

Wall shear stress demonstrated in the graphical Figures 5.1, 5.2, 5.3 and 5.4 aimed at some values of parameter for hall and ion slip on wavy channel. wall shear stress coefficient through hall and ion slip parameter for some values of M at H_1 *and* H_2. It is noticed that skin friction τ at both H_1 *and* H_2 decreases due to rise in the hall and ion slip parameter α_e *and* α_i.

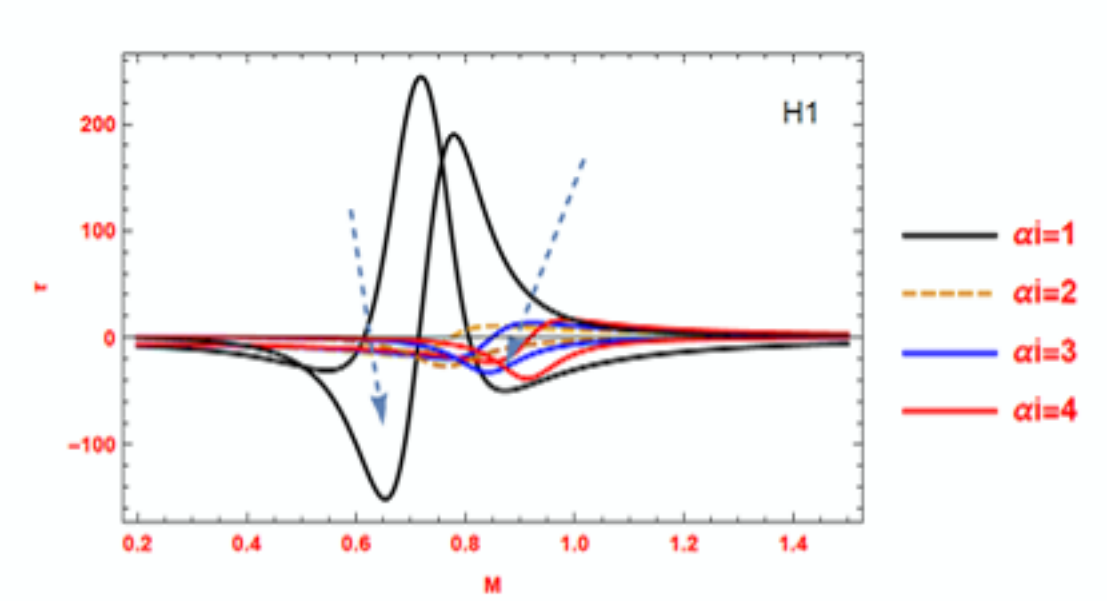

Figure 5.1

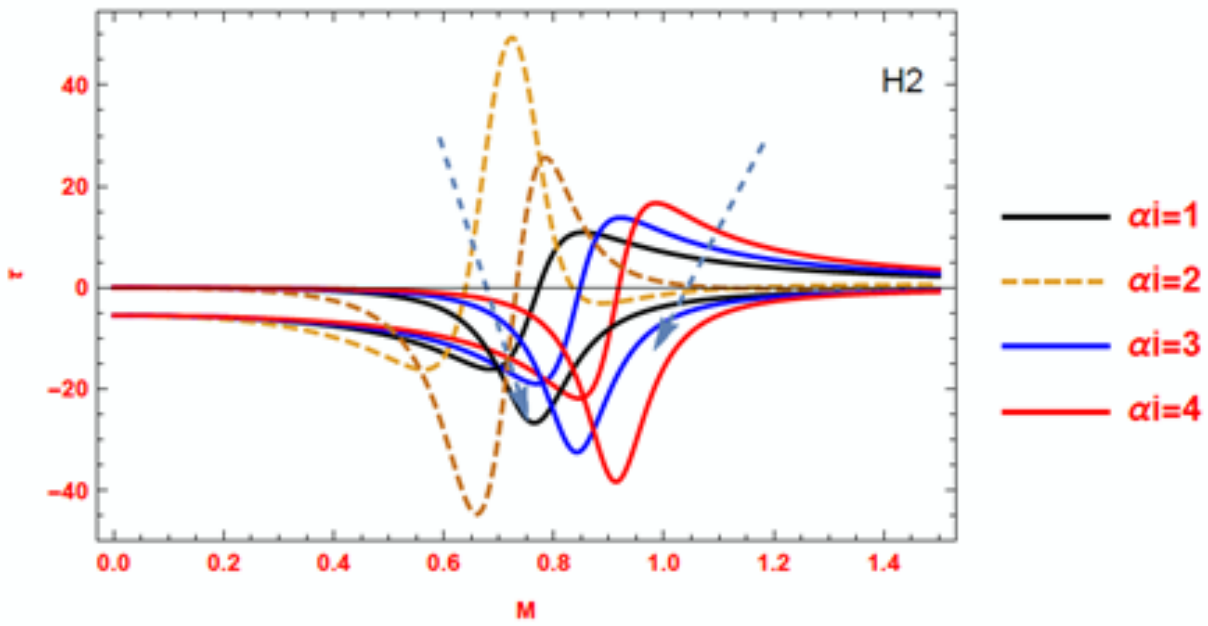

Figure 5.2

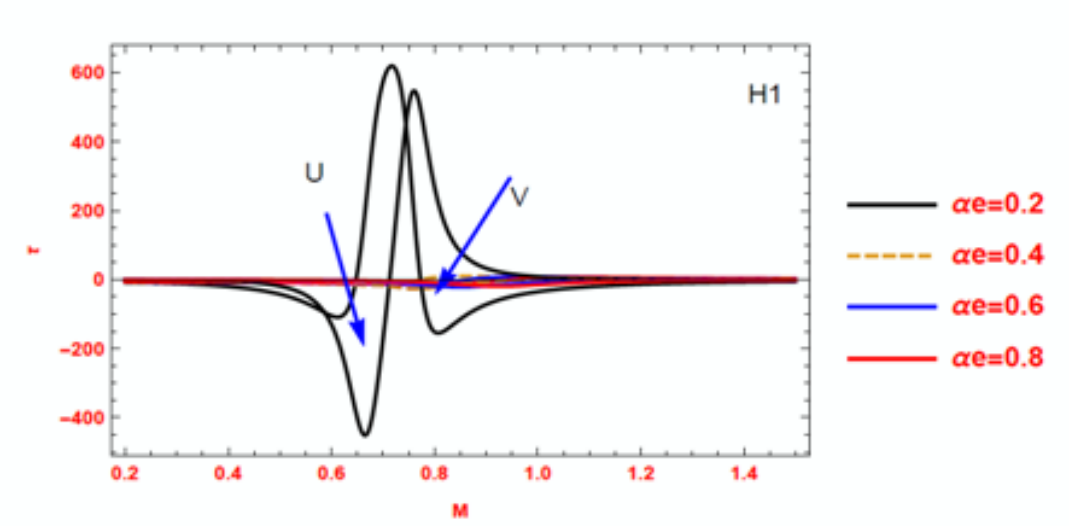

Figure 5.3

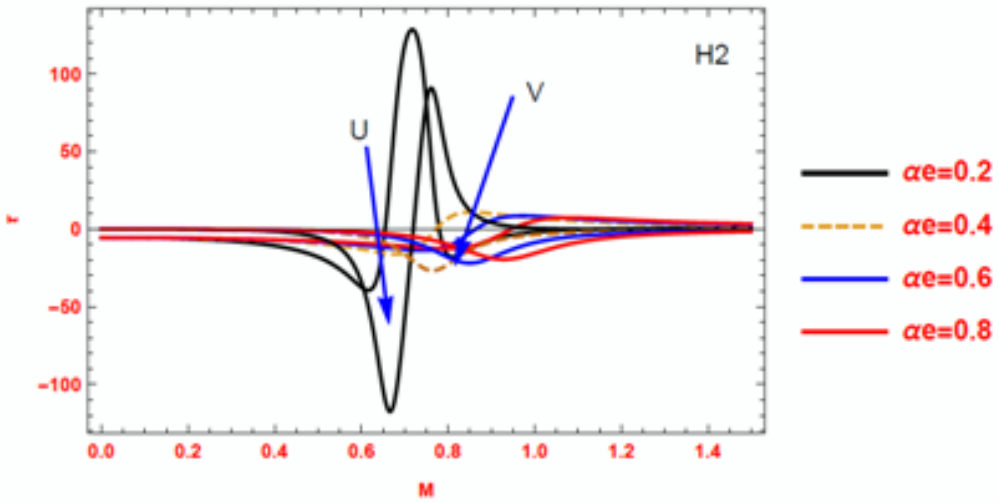

Figure 5.4

Effect of α_e *and* α_i *on* Skin friction τ

4.5 The graphical explanation of Nusselt number Nu:

Nusselt number displayed in the graphical Figures 6.1, 6.2, 6.3 and 6.4 for some values of radiation parameter R also heat generation parameter Q. As the result of the graphs in which radiation and heat generation notably partake an effect on the temperature fields and hence it disturbs the Nusselt

number. So thatthis can be indisputable from graph that Nusselt number increases in value of R and Q at both Influences

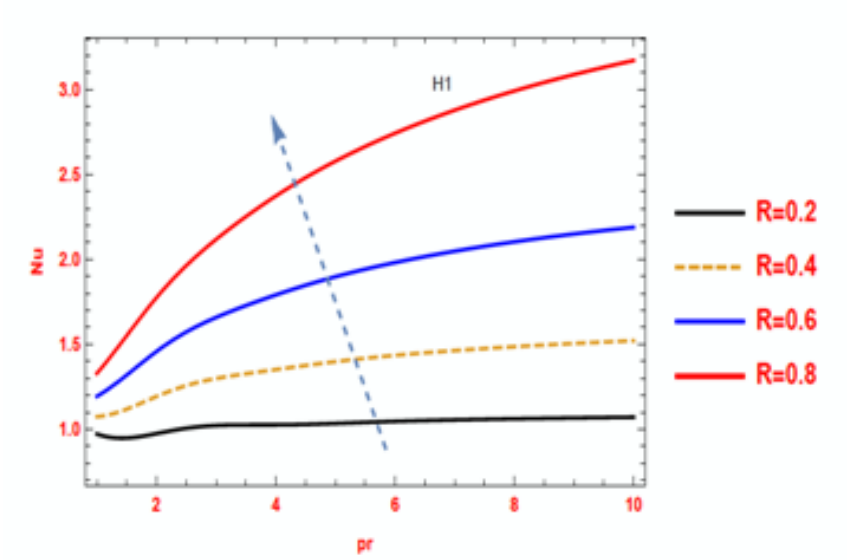

Figure 6.1

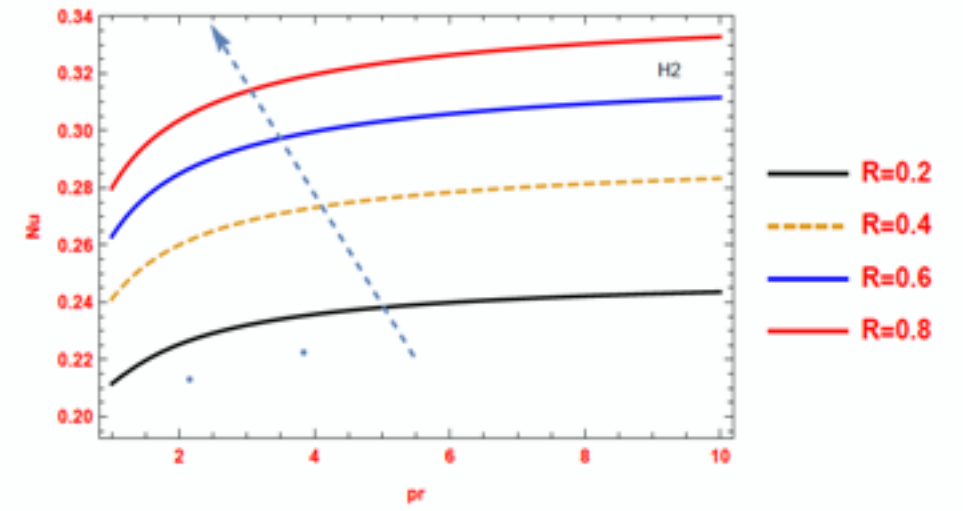

Figure 6.2

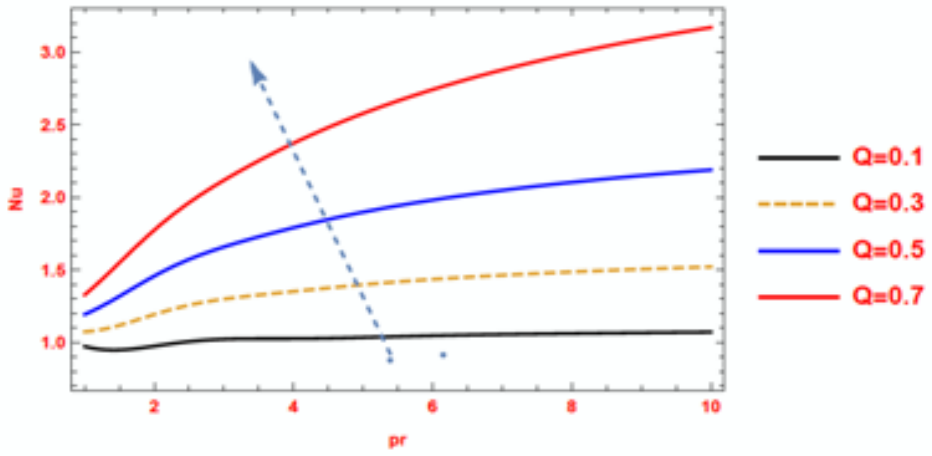

Figure 6.3

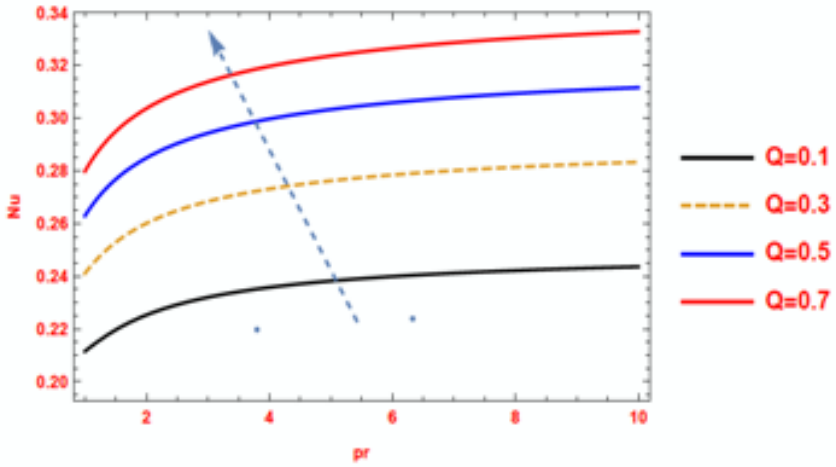

Figure 6.4

4.6 The graphical explanation of Sherwood number Sh:

Sherwood number depicted in the graphical Figures 7.1 and 7.2 for the value of Schmidt number. Sherwood number exposes by means of the variation of mass transfer Sherwood number for dissimilar quantities of Schmidt number Sc at the wall It is understandable from the figure that Sherwood number Sh at both

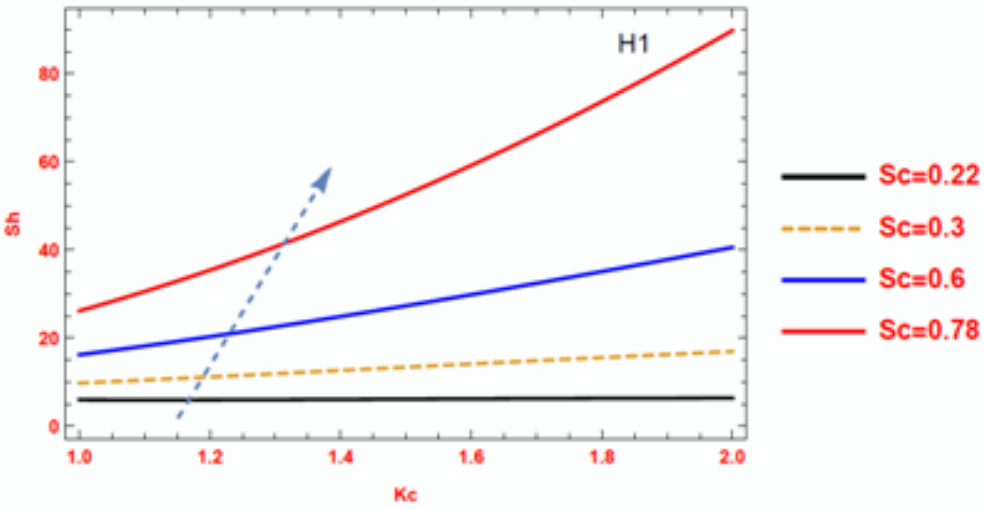

Figure 7.1

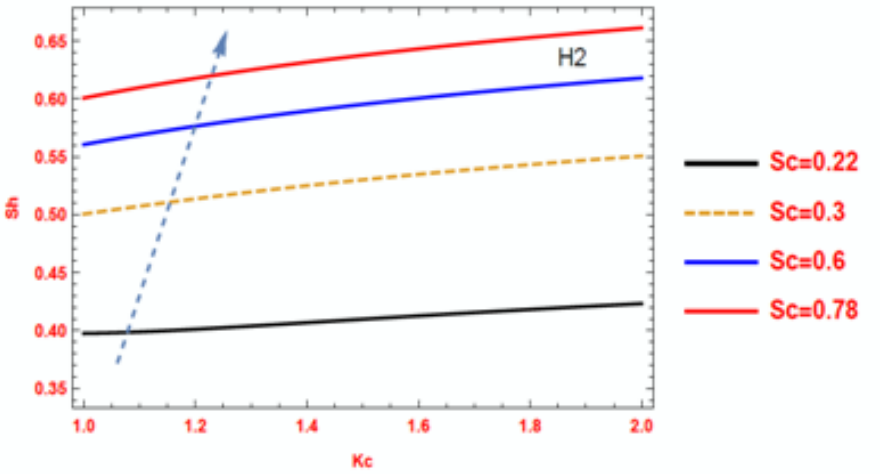

Figure 7.2

Effect of *Sc on* Sherwood number Sh

5. Conclusions

This discussion shows a mathematical ideal for two-dimensional magnetohydrodynamics current of Casson fluid peristaltic transport an unsteady surface through a porous materialwith chemical reaction.

From this investigation, we summarise the conclusion following:

- There exists intersection by maximum direction over the channel centreline and minimum direction on the walls are in the fluid velocity profile.
- The problem is very interesting that the velocity profile augments through mounting in Hartman number in both the region.
- Hall effect, radiation and heat generation parameter induce a rise in secondary velocity and lessen in the primary velocity whereas ion slip effect, chemical reaction and mass Grashof number are just opposite to it. But thermal Grashof number maintain the same length with the mount values.
- In due with chemical reaction the concentration profile studied as the fluid motion retardedness. Hence the concentration which in turn lessens as well as augments effects of Schmidt number, chemical reaction and mass transfer Biot number.
- The heat is transported to the system by a few orders of magnitude so the oscillatory flow varies due to varies quantities of different parameters of conduction. Radiation and heat generation parameter are similar expression whereas Prandtl number and thermal transfer Biot number differ from the above.
- For increasing Prandtl numbers and chemical reaction parameter values at both walls, the Nusselt and Sherwood numbers can be mounted.
- Consequence of the wall shear stress reductions took place while parameter for hall and ion slip is increased at length of the wall y = when hall and ion slip released the face effect on the wall shear stress at the wall.

APPENDIX

$\beta_I = \frac{1+\alpha_e\alpha_i}{(1+\alpha_e\alpha_i)^2+\alpha_e^2}$; $\beta_{II} = \frac{\alpha_e}{(1+\alpha_e\alpha_i)^2+\alpha_e^2}$; $m_7 = \frac{Sc+\sqrt{Sc^2+4S_{11}}}{2}$; $m_8 = \frac{Sc-\sqrt{Sc^2+4S_{11}}}{2}$;

$h_1 = 1 + a\cos[2\pi x]$; $h_2 = -d - b\cos[2\pi x + \varphi]$; $m_9 = \frac{S_{30}+\sqrt{S_{30}{}^2+4S_{31}}}{2}$; $m_{10} = \frac{S_{30}-\sqrt{S_{30}{}^2+4S_{31}}}{2}$;

$m_1 = \frac{R_1\mathrm{pr}+\sqrt{pr^2R_1{}^2+4s_1}}{2}$; $m_2 = \frac{R_1\mathrm{pr}+\sqrt{pr^2R_1{}^2+4s_1}}{2}$; $m_{11} = \frac{S_{50}+\sqrt{S_{50}{}^2+4S_{51}}}{2}$; $m_{12} = \frac{S_{50}-\sqrt{S_{50}{}^2+4S_{51}}}{2}$;

$m_3 = \frac{\mathrm{pr}+\sqrt{pr^2+4S_6}}{2}$; $m_4 = \frac{R_1\mathrm{pr}-\sqrt{pr^2+4S_6}}{2}$; $A_1 = \frac{bhS_3}{S_3S_4-S_2S_5}$; $A_2 = \frac{bhS_2}{S_3S_4-S_2S_5}$;

$m_5 = \frac{R_1Sc+\sqrt{Sc^2R_1{}^2+4KrSc}}{2}$; $m_6 = \frac{R_1Sc-\sqrt{Sc^2R_1{}^2+4KrSc}}{2}$;

$A_3 = \frac{S_{24}S_{25}-S_{22}S_{27}}{S_{22}S_{26}-S_{23}S_{25}}$; $A_4 = \frac{S_{24}S_{26}-S_{23}S_{27}}{S_{22}S_{26}-S_{23}S_{25}}$; $A_{11} = \frac{S_{64}A_{12}+S_{65}}{S_{63}}$; $A_{12} = \frac{S_{65}S_{66}-S_{63}S_{68}}{S_{63}S_{67}-S_{64}S_{66}}$;

$A_5 = \frac{bhS_8}{S_8S_9-S_7S_{10}}$; $A_6 = \frac{bhS_7}{S_8S_9-S_7S_{10}}$; $S_1 = (R+Q)P_r$; $S_2 = e^{m_1h_1}(m_1 - b_h)$;

$A_7 = \frac{S_{16}S_{18}-S_{15}S_{19}}{S_{14}S_{18}-S_{15}S_{17}}$; $A_8 = \frac{S_{16}S_{17}-S_{14}S_{19}}{S_{14}S_{18}-S_{15}S_{17}}$; $S_3 = e^{-m_2h_1}(m_2 + b_h)$; $S_4 = e^{m_1h_2}(m_1 + b_h)$;

$A_9 = \frac{S_{43}A_{10}-S_{44}}{S_{42}}$; $A_{10} = \frac{S_{45}S_{44}-S_{42}S_{47}}{S_{46}S_{42}-S_{45}S_{43}}$; $S_5 = e^{-m_2h_2}(m_2 - b_h)$; $S_6 = -P_r(R_1iw + S_1)$;

$$A_{11} = \frac{S_{64}A_{12}+S_{65}}{S_{63}}; \quad A_{12} = \frac{S_{65}S_{66}-S_{63}S_{68}}{S_{63}S_{67}-S_{64}S_{66}}; \quad S_{27} = e^{m_2h_2}S_{20}(m_1-b_h) - e^{-m_2h_2}S_{21}(m_2-b_h);$$

$$S_1 = (R+Q)P_r; \quad S_2 = e^{m_1h_1}(m_1-b_h); \quad S_{28} = M^2(\alpha_{11}+\alpha_{22}) + \sigma^2; \quad S_{29} = 1+\frac{1}{\beta_c};$$

$$S_3 = e^{-m_2h_1}(m_2+b_h); \quad S_4 = e^{m_1h_2}(m_1+b_h); \quad S_{30} = \frac{R_1}{S_{29}}; \quad S_{31} = \frac{S_{28}}{S_{29}};$$

$$S_5 = e^{-m_2h_2}(m_2-b_h); \quad S_6 = -P_r(R_1iw+S_1); \quad S_{32} = \frac{\lambda e^{i\omega t}}{S_{29}}; \quad S_{33} = \frac{A_5G_c}{S_{29}};$$

$$S_7 = e^{m_5h_1}(m_5-b_m); \quad S_8 = e^{-m_6h_1}(m_6-b_m); \quad S_{34} = \frac{A_6G_c}{S_{29}}; \quad S_{35} = \frac{A_1G_r}{S_{29}};$$

$$S_9 = e^{m_5h_2}(m_5-b_m); \quad S_{10} = e^{-m_6h_2}(m_6-b_m);$$

$$S_{11} = Sc(k_r+R_1i\omega); \quad S_{12} = \frac{A_5}{m_5^2-SCm_5-S_{11}};$$

$$S_{13} = \frac{A_6}{m_6^2+SCm_6-S_{11}}; \quad S_{14} = e^{m_7h_1}(m_7-b_m);$$

$$S_{15} = e^{-m_8h_1}(m_8+b_m); \quad S_{16} = e^{m_5h_1}S_{12}(m_5-b_m) - e^{m_6h_1}S_{13}(m_6-b_m);$$

$$S_{17} = e^{m_7h_2}(m_7-b_m); \quad S_{18} = e^{-m_8h_2}(m_8+b_m);$$

$$S_{19} = e^{m_6h_2}S_{12}(m_5-b_m) - e^{-m_6h_2}S_{13}(m_6-b_m);$$

$$S_{20} = \frac{A_1}{m_1^2-P_rm_1-S_6}; \quad S_{21} = \frac{-A_2}{m_2^2+P_rm_2-S_6};$$

$$S_{22} = e^{m_3h_1}(m_3-b_h); \quad S_{23} = e^{-m_3h_1}(m_4+b_h);$$

$$S_{24} = e^{m_1h_1}S_{20}(m_1-b_h) - e^{-m_2h_1}S_{21}(m_2-b_h);$$

$$S_{25} = e^{m_3h_2}(m_3-b_h); \quad S_{26} = e^{-m_4h_2}(m_4+b_h);$$

$$S_{36} = \frac{A_2G_r}{S_{29}}; \quad S_{37} = -\frac{S_{32}}{S_{31}};$$

$$S_{38} = -\frac{S_{33}}{m_5^2-S_{30}m_5-S_{31}}; \quad S_{39} = -\frac{S_{34}}{m_6^2+S_{30}m_6-S_{31}};$$

$$S_{40} = -\frac{S_{35}}{m_1^2-S_{30}m_1-S_{31}}; \quad S_{41} = -\frac{S_{36}}{m_2^2+S_{30}m_2-S_{31}};$$

$$S_{42} = e^{m_9h_1}\left(m_9-\alpha_f\sigma\right); \quad S_{43} = e^{-m_{10}h_1}\left(m_{10}+\alpha_f\sigma\right);$$

$$S_{44} = -S_{38}m_5e^{m_5h_1} + S_{39}m_6e^{-m_6h_1} - S_{40}m_1e^{-m_1h_1} + S_{41}m_2e^{-m_2h_1} + \alpha_f\sigma(S_{37}+S_{38}e^{m_5h_1}+S_{39}e^{-m_6h_1}+S_{40}e^{-m_1h_1}+S_{41}e^{-m_2h_1});$$

$$S_{45} = e^{m_9h_2}\left(m_9+\alpha_f\sigma\right); \quad S_{46} = e^{-m_{10}h_2}\left(m_{10}-\alpha_f\sigma\right);$$

$$S_{47} = -S_{38}m_5e^{m_5h_2} + S_{39}m_6e^{-m_6h_1} - S_{40}m_1e^{-m_1h_2} + S_{41}m_2e^{-m_2h_2} - \alpha_f\sigma(S_{37}+S_{38}e^{m_5h_2}+S_{39}e^{-m_6h_2}+S_{40}e^{m_1h_2}+S_{41}e^{-m_2h_2});$$

$$S_{50} = \frac{R_1}{S_{28}}; \quad S_{51} = \frac{S_{29}+R_1\epsilon i\omega}{S_{28}};$$

$$S_{52} = \frac{G_c}{S_{28}}; \quad S_{53} = \frac{G_r}{S_{28}};$$

$$S_{54} = \frac{A_9S_{50}m_9}{m_9^2-S_{50}m_9-S_{51}}; \quad S_{55} = \frac{A_{10}S_{50}m_{10}}{m_{10}^2+S_{50}m_{10}-S_{51}};$$

$$S_{58} = \frac{S_{53}A_3}{m_3^2 - S_{50}m_3 - S_{51}}; \qquad S_{59} = \frac{S_{50}S_{38}m_5 - S_{52}S_{12}}{m_5^2 - S_{50}m_5 - S_{51}};$$

$$S_{60} = \frac{S_{50}S_{39}m_6 + S_{52}S_{13}}{m_6^2 + S_{50}m_6 - S_{51}}; \qquad S_{61} = \frac{S_{50}S_{40}m_1 - S_{53}S_{20}}{m_1^2 - S_{50}m_1 - S_{51}};$$

$$S_{62} = \frac{S_{50}S_{41}m_1 - S_{53}S_{21}}{m_2^2 + S_{50}m_6 - S_{51}}; \qquad S_{63} = e^{m_{11}h_1}\left(m_{11} - \alpha_f\sigma\right);$$

$$S_{64} = e^{-m_{12}h_1}\left(m_{12} + \alpha_f\sigma\right);$$

$$\begin{aligned} S_{65} = &-S_{54}m_9e^{m_9h_1} - S_{55}m_{10}e^{-m_{10}h_1} + S_{56}m_7e^{m_7h_1} - S_{57}m_8e^{-m_8h_1} + S_{58}m_3e^{m_3h_1} - S_{59}m_5e^{-m_5h_1} \\ &- S_{60}m_6e^{-m_6h_1} - S_{61}m_1e^{m_1h_1} - S_{62}m_2e^{-m_2h_1} \\ &+ \alpha_f\sigma(S_{54}e^{m_9h_1} - S_{55}e^{-m_{10}h_1} - S_{56}e^{m_7h_1} - S_{57}e^{-m_8h_1} - S_{58}e^{m_3h_1} + S_{59}e^{-m_5h_1} \\ &- S_{60}e^{-m_6h_1} + S_{61}e^{m_1h_1} - S_{62}e^{-m_2h_1}); \end{aligned}$$

$$S_{66} = e^{m_{11}h_2}\left(m_{11} + \alpha_f\sigma\right); \qquad S_{67} = e^{-m_{12}h_2}\left(m_{12} - \alpha_f\sigma\right);$$

$$\begin{aligned} S_{68} = &-S_{54}m_9e^{m_9h_2} - S_{55}m_{10}e^{-m_{10}h_2} + S_{56}m_7e^{m_7h_2} - S_{57}m_8e^{-m_8h_2} + S_{58}m_3e^{m_3h_2} - S_{59}m_5e^{-m_5h_2} \\ &- S_{60}m_6e^{-m_6h_2} - S_{61}m_1e^{m_1h_2} - S_{62}m_2e^{-m_2h_2} \\ &- \alpha_f\sigma(S_{54}e^{m_9h_2} - S_{55}e^{-m_{10}h_2} - S_{56}e^{m_7h_2} - S_{57}e^{-m_8h_2} - S_{58}e^{m_3h_2} + S_{59}e^{-m_5h_2} \\ &- S_{60}e^{-m_6h_2} + S_{61}e^{m_1h_2} - S_{62}e^{-m_2h_2}); \end{aligned}$$

References

[1] J. R. Keltner, M. S. Roos, P. R. Brakeman, and T. F. Budinger, "Magnetohydrodynamics of blood flow," *Magn. Reson. Med.*, vol. 16, no. 1, pp. 139–149, 1990, doi: 10.1002/mrm.1910160113.

[2] N. Mustapha, N. Amin, S. Chakravarty, and P. K. Mandal, "Unsteady magnetohydrodynamic blood flow through irregular multi-stenosed arteries," *Comput. Biol. Med.*, vol. 39, no. 10, pp. 896–906, 2009, doi: 10.1016/j.compbiomed.2009.07.004.

[3] D. S. Sankar and U. Lee, "FDM analysis for MHD flow of a non-Newtonian fluid for blood flow in stenosed arteries †," vol. 25, no. 10, pp. 23–25, 2011, doi: 10.1007/s12206-011-0728-x.

[4] S. Asghar, Q. Hussain, T. Hayat, and F. Alsaadi, "Hall and ion slip effects on peristaltic flow and heat transfer analysis with Ohmic

heating," *Appl. Math. Mech. (English Ed.*, vol. 35, no. 12, pp. 1509–1524, 2014, doi: 10.1007/s10483-014-1881-6.

[5] S. Asghar, Q. Hussain, and A. Alsaedi, "Effects of Hall Current and Ion Slip in Peristalsis with Temperature-Dependent Viscosity," pp. 1–16, 2015, doi: 10.1061/(ASCE)AS.1943-5525.0000586.

[6] M. M. Bhatti and M. A. Abbas, "Simultaneous effects of slip and MHD on peristaltic blood flow of Jeffrey fluid model through a porous medium," *ALEXANDRIA Eng. J.*, pp. 4–10, 2016, doi: 10.1016/j.aej.2016.03.002.

[7] M. M. Bhatti, M. A. Abbas, and M. M. Rashidi, "Engineering Science and Technology , an International Journal Combine effects of Magnetohydrodynamics (MHD) and partial slip on peristaltic Blood flow of Ree – Eyring fluid with wall properties þ," *Eng. Sci. Technol. an Int. J.*, pp. 0–5, 2016, doi: 10.1016/j.jestch.2016.05.004.

[8] F. Ali, N. A. Sheikh, I. Khan, and M. Saqib, "Author ' s Accepted Manuscript model," *J. Magn. Magn. Mater.*, 2016, doi: 10.1016/j.jmmm.2016.09.125.

[9] Q. Hussain, S. Asghar, and A. Alsaedi, "Heat transfer analysis in peristaltic slip ow with Hall and ion-slip currents," *Sci. Iran.*, vol. 23, no. 6, pp. 2771–2783, 2016, doi: 10.24200/sci.2016.3987.

[10] M. M. Rashidi, Z. Yang, M. M. Bhatti, and M. A. Abbas, "HEAT AND MASS TRANSFER ANALYSIS ON MHD BLOOD FLOW OF CASSON FLUID MODEL DUE TO PERISTALTIC WAVE," vol. 22, no. 6, pp. 2439–2448, 2018.

[11] S. Maiti, S. Shaw, and G. C. Shit, "Pr p ro of," *Physica A*, 2019, doi: 10.1016/j.physa.2019.123149.

[12] A. Khalid, I. Khan, and S. Shafie, "Exact Solutions for Unsteady Free Convection Flow of Casson Fluid over an Oscillating Vertical Plate with Constant Wall Temperature," vol. 2015.

[13] M. Senapati, S. K. Parida, K. Swain, and S. M. Ibrahim, "Analysis of variable magnetic field on chemically dissipative MHD boundary layer flow of Casson fluid over a nonlinearly stretching sheet with slip conditions," *Int. J. Ambient Energy*, vol. 0, no. 0, pp. 1–27, 2020, doi: 10.1080/01430750.2020.1831601.

[14] S. Das, T. K. Pal, R. N. Jana, and B. Giri, "Ascendancy of electromagnetic force and Hall currents on blood flow carrying Cu-Au NPs in a non-uniform endoscopic annulus having wall slip," *Microvasc.*

Res., vol. 138, no. June, p. 104191, 2021, doi: 10.1016/j.mvr.2021.104191.

[15] H. V. C. Rajashekhar, K. V. P. S. U. Khan, F. M. Oudina, and A. P. P. Nagathan, "Channel flow of MHD bingham fluid due to peristalsis with multiple chemical reactions : an application to blood flow through narrow arteries," *SN Appl. Sci.*, vol. 3, no. 2, pp. 1–12, 2021, doi: 10.1007/s42452-021-04143-0.

[16] M Anusha Bai, "Effects of Slip and Hall on the Peristaltic Transport of a Hyperbolic Tangent Fluid in a Planar Channel," *Int. J. Eng. Res.*, vol. V8, no. 12, pp. 562–569, 2019, doi: 10.17577/ijertv8is120290.

[17] C. Vasudev, U. Rajeswara Rao, M. V. Subha Reddy, and G. Prabhakara Rao, "Effect of heat transfer on peristaltic transport of a newtonian fluid through a porous medium in an asymmetric vertical channel," *Eur. J. Sci. Res.*, vol. 44, no. 1, pp. 79–92, 2010.

[18] P. V. Satya Narayana, B. Venkateswarlu, and B. Devika, "Chemical reaction and heat source effects on MHD oscillatory flow in an irregular channel," *Ain Shams Eng. J.*, vol. 7, no. 4, pp. 1079–1088, 2016, doi: 10.1016/j.asej.2015.07.012.

[19] T. Hayat, S. Asghar, A. Tanveer, and A. Alsaedi, "Effects of Hall current and ion-slip on the peristaltic motion of couple stress fluid with thermal deposition," *Neural Comput. Appl.*, vol. 31, no. 1, pp. 117–126, 2019, doi: 10.1007/s00521-017-2984-x.

[20] J. R. Pattnaik, G. C. Dash, and S. Singh, "Radiation and mass transfer effects on MHD flow through porous medium past an exponentially accelerated inclined plate with variable temperature," *Ain Shams Eng. J.*, vol. 8, no. 1, pp. 67–75, Mar. 2017, doi: 10.1016/j.asej.2015.08.014.

[21] W. G. England and A. F. Emery, "Thermal radiation effects on the laminar free convection boundary layer of an absorbing gas," *J. Heat Transfer*, vol. 91, no. 1, pp. 37–44, 1969, doi: 10.1115/1.3580116.

[22] I. M. I. Eldesoky, "Unsteady MHD pulsatile blood flow through porous medium in stenotic channel with slip at permeable walls subjected to time dependent velocity (injection/suction)," *Walailak J. Sci. Technol.*, vol. 11, no. 11, pp. 901–922, 2014, doi: 10.21608/icmep.2014.29736.

[23] M. V. Krishna, "Hall and ion slip effects on radiative MHD rotating flow of Jeffreys fluid past an infinite vertical flat porous surface with ramped wall velocity and temperature," *Int. Commun. Heat Mass Transf.*, vol. 126, p. 105399, 2021, doi: 10.1016/j.icheatmasstransfer.2021.105399.

[24] M. Veera Krishna, N. Ameer Ahamad, and A. J. Chamkha, "Hall and ion slip impacts on unsteady MHD convective rotating flow of heat generating/absorbing second grade fluid," *Alexandria Eng. J.*, vol. 60, no. 1, pp. 845–858, 2021, doi: 10.1016/j.aej.2020.10.013.

[25] M. V. Krishna, N. A. Ahamad, and A. J. Chamkha, "Hall and ion slip impacts on unsteady MHD convective rotating flow of heat generating / absorbing second grade fluid," *Alexandria Eng. J.*, 2020, doi: 10.1016/j.aej.2020.10.013.